

Supporting Information

for

High-Effective Gene Delivery Based on Cyclodextrins Multivalent Assembly in Target Cancer Cells

Yao-Hua Liu, Yu Liu*

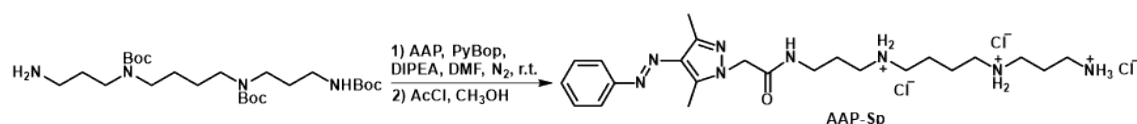
College of Chemistry, State Key Laboratory of Elemento-Organic Chemistry, Nankai
University, Tianjin 300071, P. R. China

*E-mail: yuliu@nankai.edu.cn

Instruments. NMR spectra were recorded on Bruker 400 MHz instrument, and chemical shifts were recorded in parts per million (ppm). High resolution mass (HRMS) spectra were performed on Varian 7.0T FTMS with ESI or MALDI source. TEM images were acquired by a high-resolution transmission electron microscope (Philips Tecnai G2 20S-TWIN microscope) operating at an accelerating voltage of 200 keV. The samples were prepared by placing a drop of solution onto a carbon-coated copper grid and air-dried. The morphological information was directly obtained from the fresh TEM samples without staining. Transmission spectra were recorded on a Shimadzu UV-3600 spectrophotometer in a quartz cell (light path 10 mm) at 37 °C with a PTC-348WI temperature controller. Dynamic light scattering (DLS) was recorded on BI-200SM (Brookhaven Company) at 37 °C. Confocal fluorescence imaging was recorded with Olympus FV1000.

Cell Culture. The human embryonic kidney normal cell line (293T cells), cervical cancer cell line (Hela cells) and human lung cancer cell line (A549 cells) were all purchased from Cell Resource Center, Chinese Academy of Medical Science Beijing. A549 cancer cells were incubated by using Ham's F12 nutrient medium supplemented with 10 % FBS and 1 % penicillin/streptomycin in a humidified incubator with 5% CO₂ atmosphere at 37 °C. 293T normal cells and Hela cells were cultured with DMEM medium containing 10 % FBS and 1 % penicillin/streptomycin in a humidified incubator with 5% CO₂ atmosphere at 37 °C.

Synthesis of AAPS



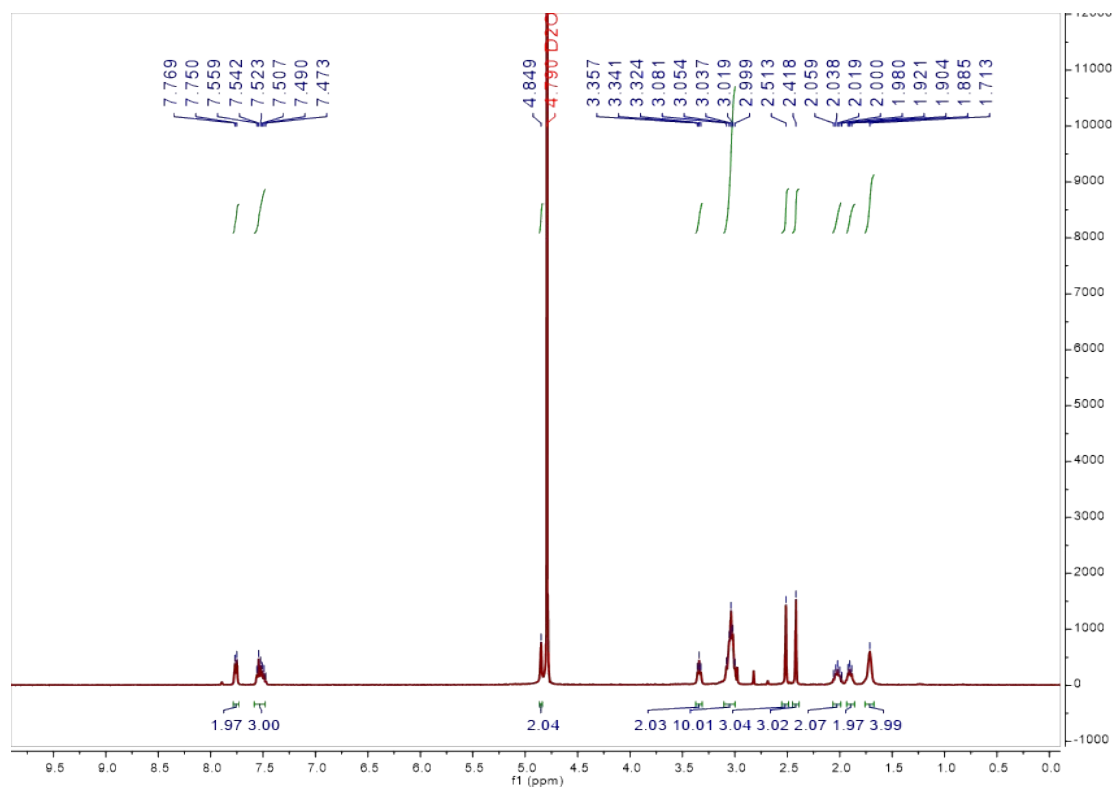


Figure S1. ^1H NMR spectra (400 MHz, D_2O , 298K) of AAPS.

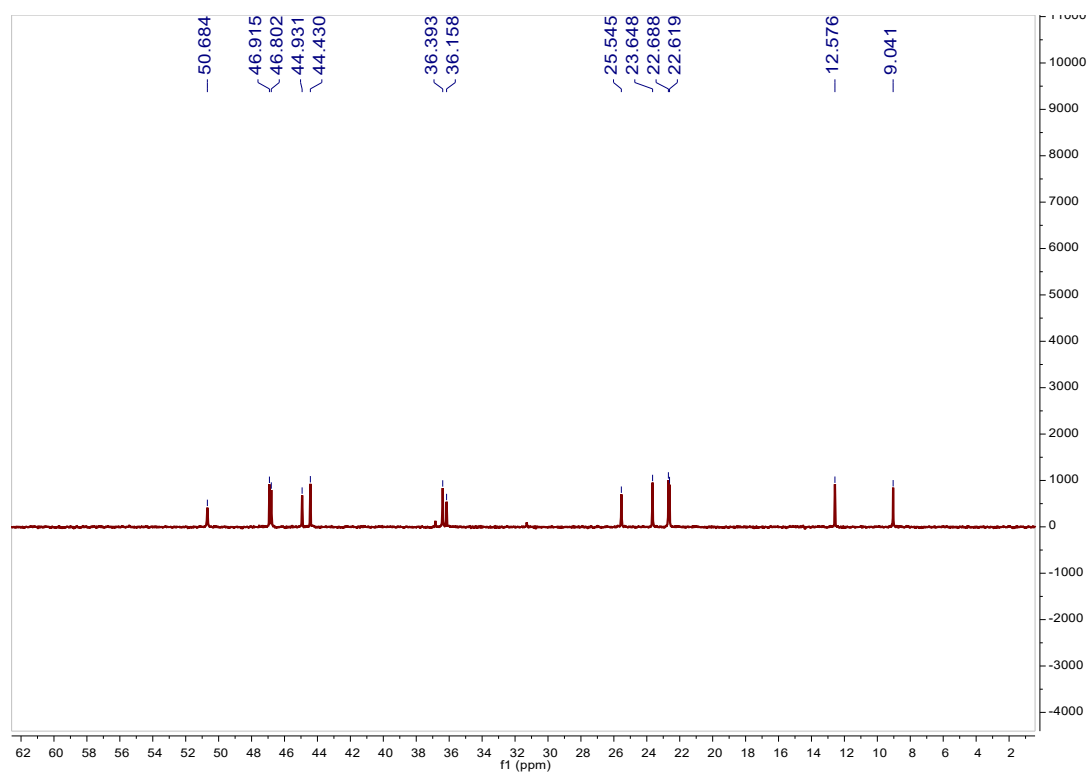


Figure S2. ^{13}C NMR spectra (101 MHz, D_2O , 298K) of AAPS.

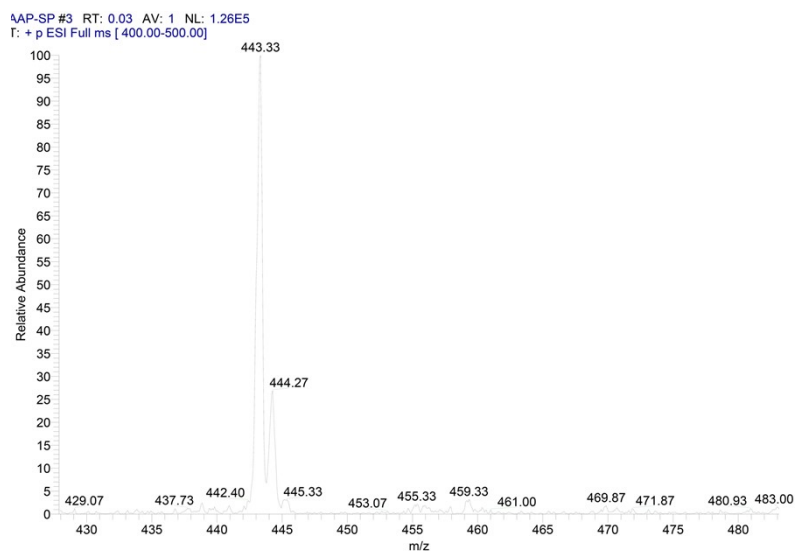


Figure S3. ESI-MS spectrum of AAPS.

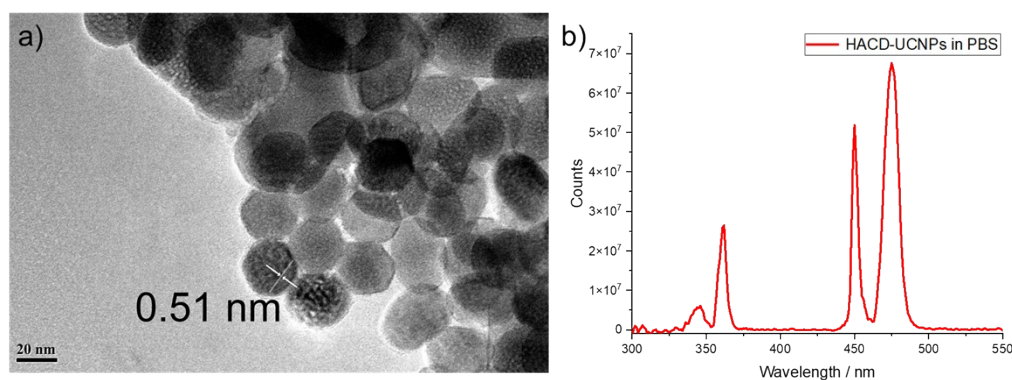


Figure S4. (a) HR-TEM image of HACD-UCNPs; (b) Photoluminescence spectrum of HACD-UCNPs excited by 980 nm in PBS (0.01 M, pH = 7.2).

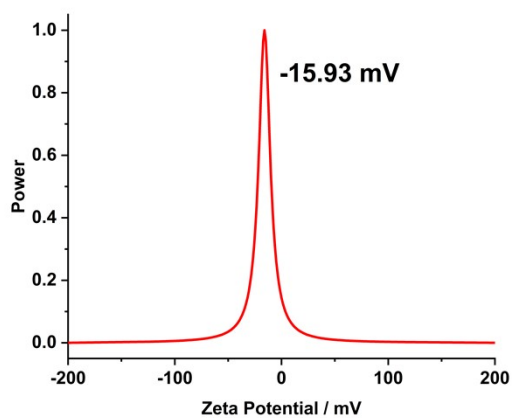


Figure S5. Zeta-potential experiment of HACD-UCNPs in PBS (0.01 M, pH = 7.2, 25

°C).

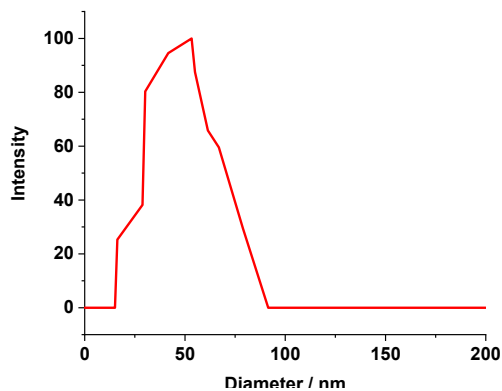


Figure S6. DLS experiment of HACD-UCNPs in PBS (0.01 M, pH = 7.2, 25 °C)

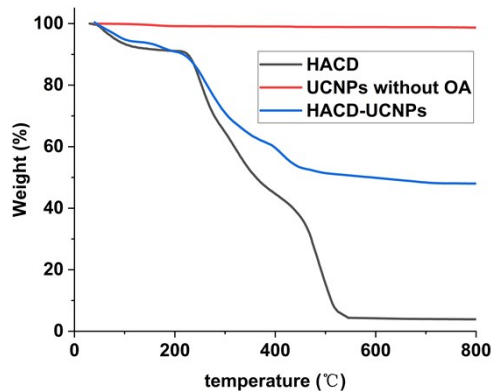


Figure S7. Thermogravimetric analysis of HACD-UCNPs from 40 to 800 °C.

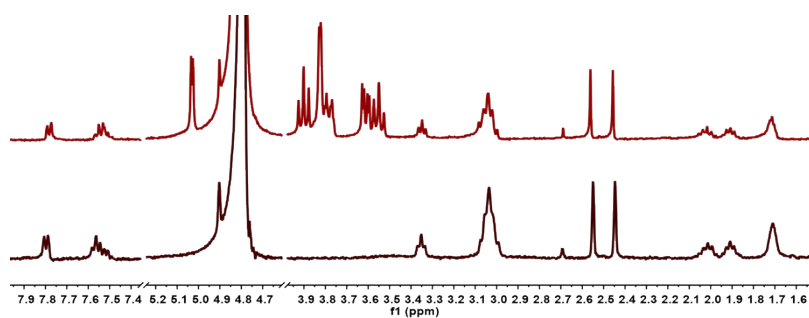


Figure S8. Partial ^1H NMR spectra (400 MHz, D_2O , 298K) of AAPS (bottom) and AAPS- β -CD (top).

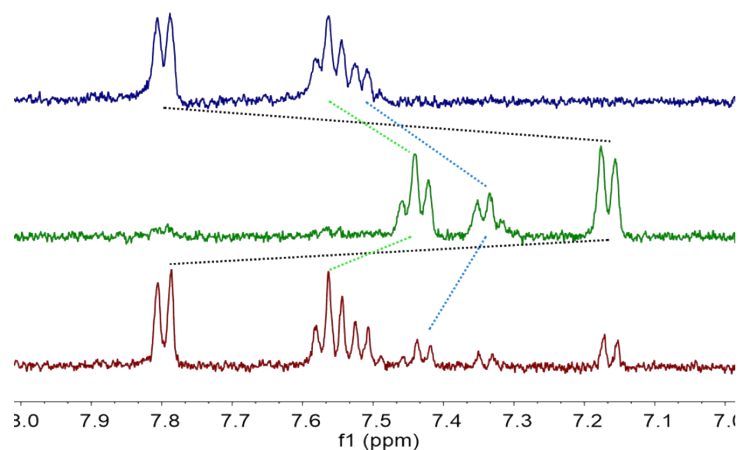


Figure S9. Partial ^1H NMR spectra (400 MHz, D_2O , 298K) of AAPS (top) with 365 nm irradiation for 10 min (middle) and 520 nm irradiation for 10 min (bottom).

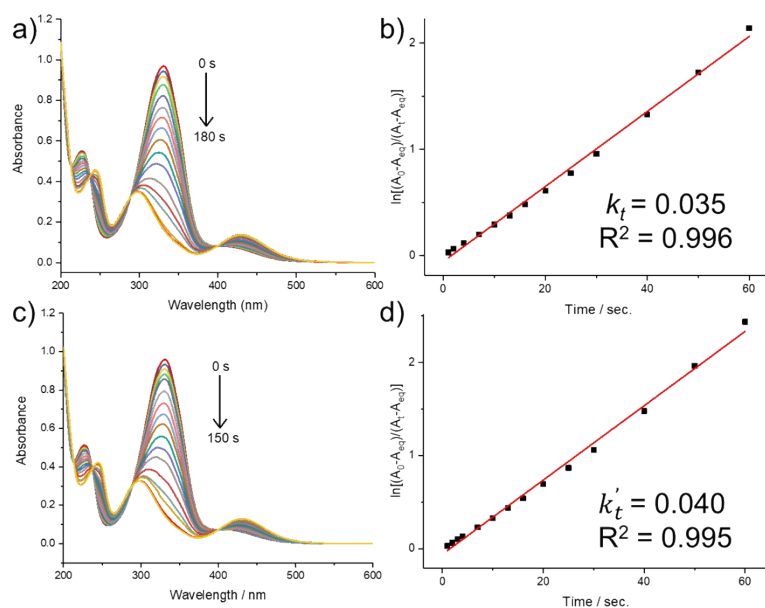


Figure S10. (a) UV-vis spectra of AAPS ($50\ \mu\text{M}$) to determine the photoisomerization rate constant (k_t) in PBS. The duration of UV light was set at 0 - 180 s at 365 nm; (b) Determination of the k_t value of AAPS upon exposure to UV light at 365 nm; (c) UV-vis spectra of AAPS- β -CD ($50\ \mu\text{M}$) to determine the photoisomerization rate constant (k_t) in PBS. The duration of UV light was set at 0 - 150 s at 365 nm; (d) Determination of the k_t value of AAPS- β -CD upon exposure to UV light at 365 nm.

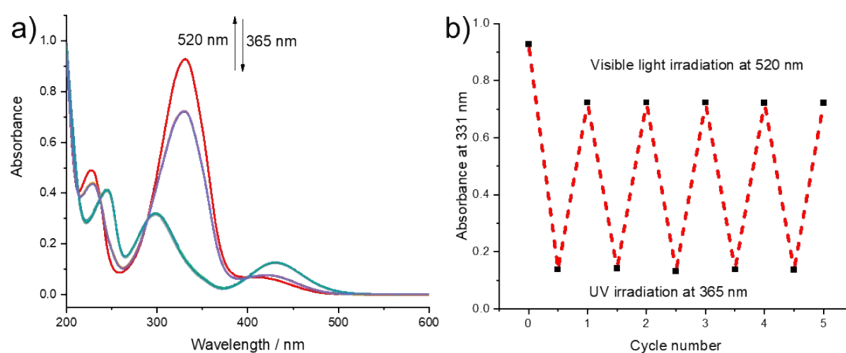


Figure S11. Cyclic responses of (a) the UV-vis spectrum and (b) the absorbance values at 331 nm of AAPS-β-CD (50 μM) on alternating irradiation between UV and visible light.

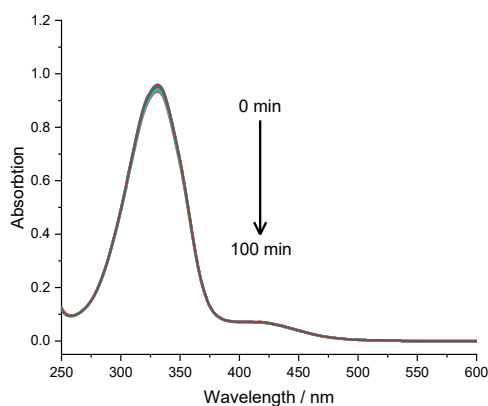


Figure S12. UV-Vis spectrum of AAPS under 980 nm light irradiation at $1 \text{ W}\cdot\text{cm}^{-2}$ in PBS ($[\text{AAPS}] = 50 \mu\text{M}$, pH 7.2, 0.01 M, 25 °C).

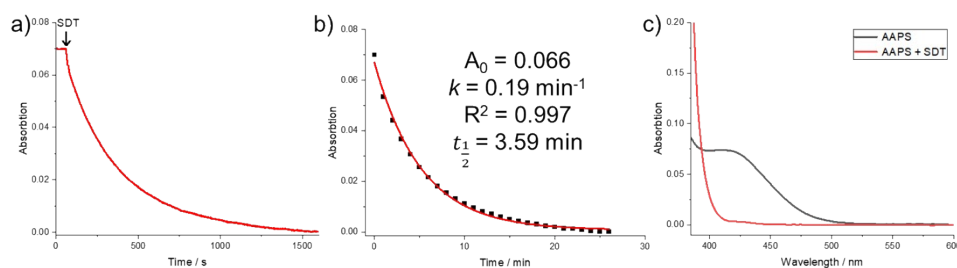


Figure S13. (a) Absorbance at 425 nm of AAPS (50 μM) as a function of time following addition of SDT (1.0 mM) and (b) the corresponding fitting curve according to quasi-first order reaction decay model; (c) Absorbance spectra of AAPS (50 μM) before and after reduction by SDT (1.0 mM).

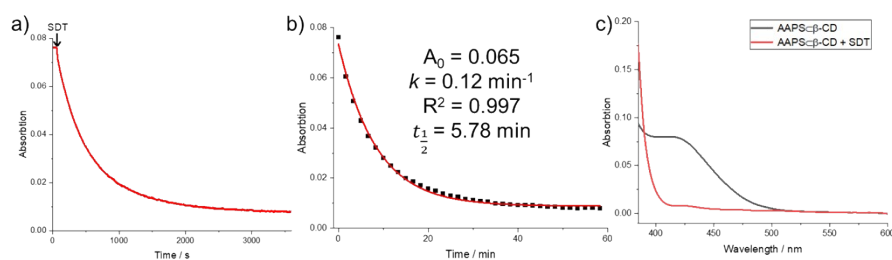


Figure S14. (a) Absorbance at 425 nm of AAPS- β -CD (50 μ M) as a function of time following addition of SDT (1.0 mM) and (b) the corresponding fitting curve according to quasi-first order reaction decay model; (c) Absorbance spectra of AAPS- β -CD (50 μ M) before and after reduction by SDT (1.0 mM).

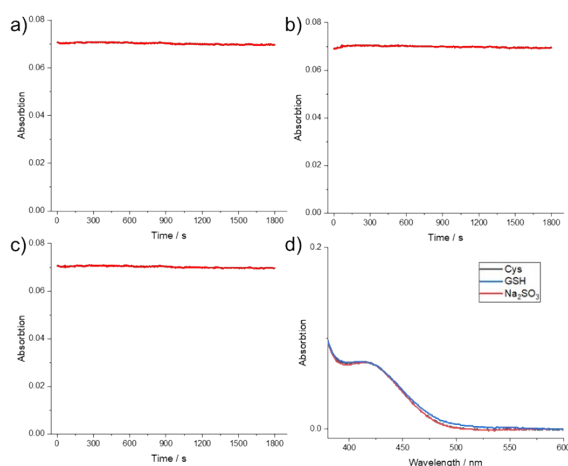


Figure S15. Absorbance at 425 nm of AAPS (50 μ M) as a function of time following addition of (a) Cys (0.1 mM), (b) GSH (0.1 mM) and (c) Na₂SO₃ (1 mM); (d) Absorbance spectra of AAPS (50 μ M) after reduction by Cys (0.1 mM), GSH (0.1 mM) and Na₂SO₃ (1 mM).

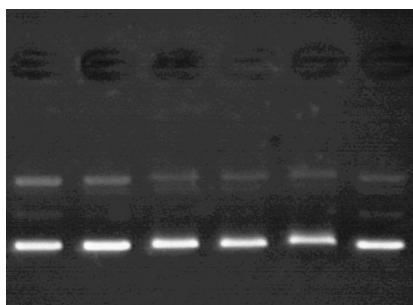


Figure S16. Agar gelatin electrophoresis of AAPS-HACD-UCNPs@pBR322 ([AAPS-HACD-UCNPs] = 30, 10, 3, 1 μ M), AAPS@pBR322 ([AAPS] = 100 μ M) and HACD-UCNPs/pBR322 ([HACD-UCNPs] = 100 μ M) from left to right (The S8

concentration of pBR322 in all groups was 10 ng/ μL).

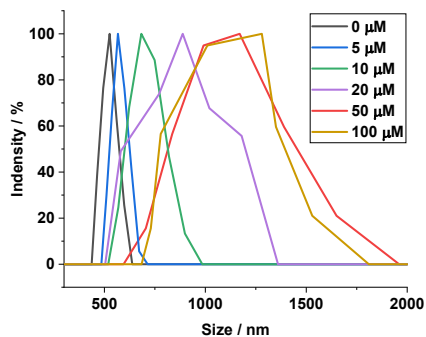


Figure S17. Diameter distributions of pBR322 ($[\text{pBR322}] = 4 \mu\text{g/mL}$) with different amounts of AAPS-HACD-UCNPs in PBS ($\text{pH} = 7.2$, 0.01 M , $25 \text{ }^\circ\text{C}$).

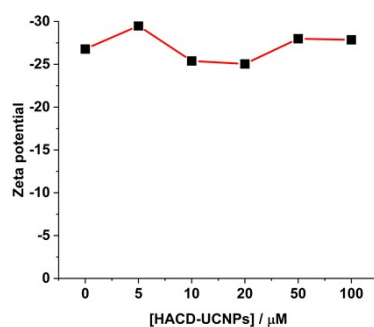


Figure S18. Zeta potentials of pBR322 ($[\text{pBR322}] = 4 \mu\text{g/mL}$) with different amounts of AAPS-HACD-UCNPs in PBS ($\text{pH} = 7.2$, 0.01 M , $25 \text{ }^\circ\text{C}$).

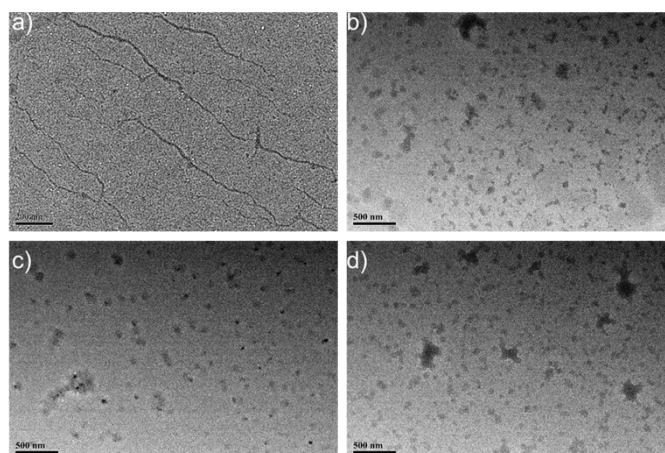


Figure S19. TEM image of (a) pBR322 and AAPS-HACD-UCNPs@pBR322 treated with (b) SDT or irradiation of (c) 365 nm for 10 min or (d) 980 nm for 30 min.

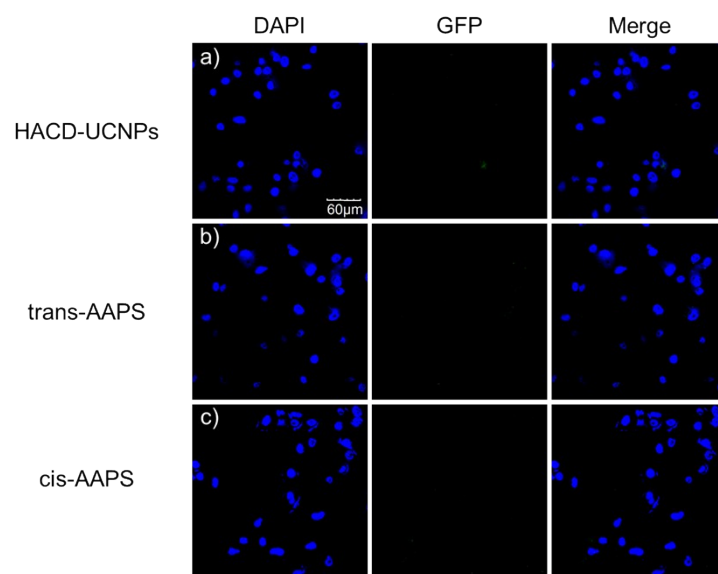


Figure S20. Confocal laser fluorescence microscope images of A549 cells cultured with (a) HACD-UCNPs/pEGFP, (b) trans-AAPS@pEGFP or (c) cis-AAPS@pEGFP.

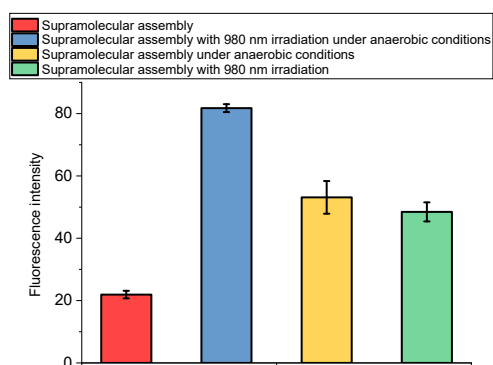


Figure S21. Average fluorescence intensity of GFP in the confocal laser images analyzed by ImageJ software (ver 1.53c).

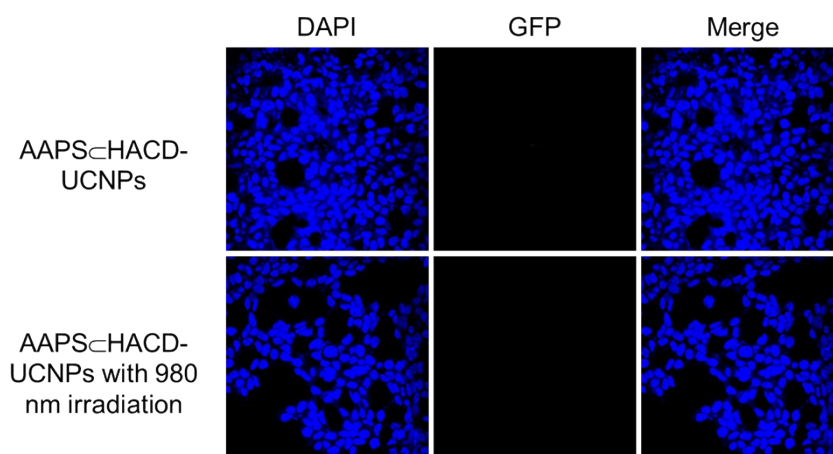


Figure S22. Confocal laser fluorescence microscope images of 293T cells cultured with

AAPS \subset HACD-UCNPs@pEGFP and AAPS \subset HACD-UCNPs@pEGFP with 980 nm irradiation for 30 min.

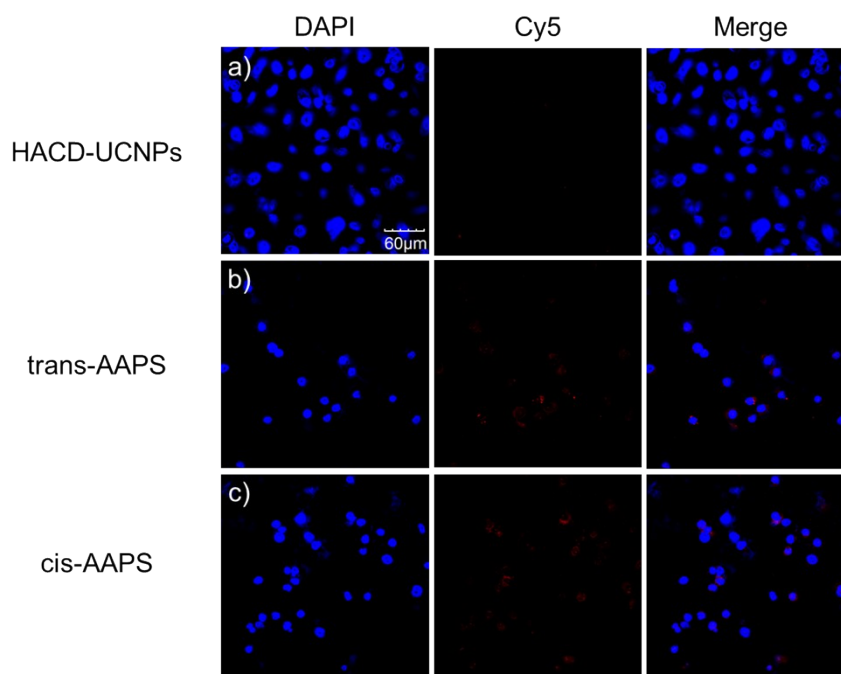


Figure S23. Confocal laser fluorescence microscope images of A549 cells cultured with (a) HACD-UCNPs/Cy5-siRNA, (b) trans-AAPS@Cy5-siRNA or (c) cis-AAPS@Cy5-siRNA.

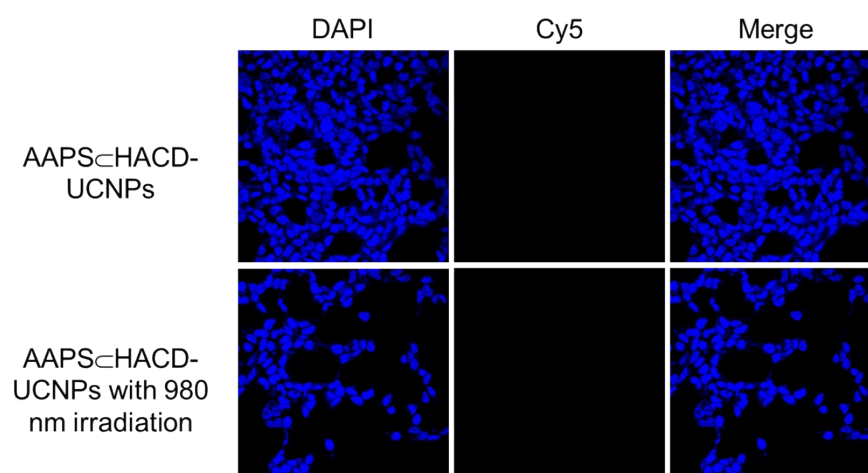


Figure S24. Confocal laser fluorescence microscope images of 293T cells cultured with AAPS \subset HACD-UCNPs@Cy5-siRNA and AAPS \subset HACD-UCNPs@Cy5-siRNA with 980 nm irradiation for 30 min.

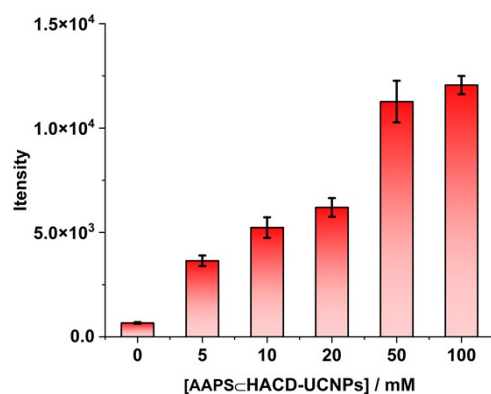


Figure S25. Red fluorescence intensity in A549 cells incubated with Cy5-siRNA and different amounts of AAPS@HACD-UCNPs. The concentration of Cy5-siRNA in all experiments was 100 nM.

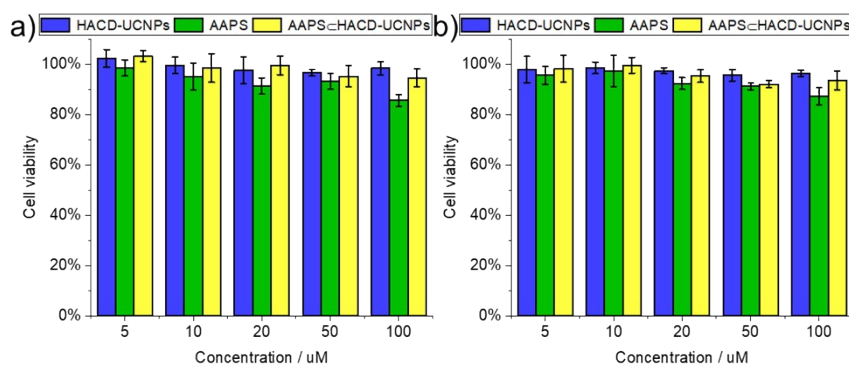


Figure S26. Cell viability of (a) HeLa and (b) 293T cells induced with HACD-UCNPs, AAPS and AAPS@HACD-UCNPs at various concentrations

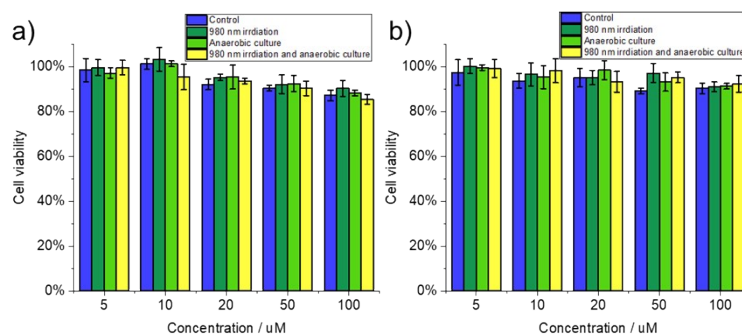


Figure S27. Cell viability of (a) A549 and (b) HeLa cells induced with AAPS@siRNA at various concentrations with different treatment. The concentration of siRNA in all experiments was 100 nM.

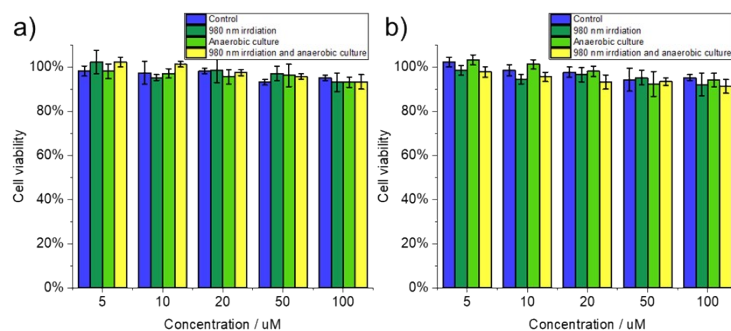


Figure S28. Cell viability of (a) A549 and (b) Hela cells induced with HACD-UCNPs/siRNA at various concentrations with different treatment. The concentration of siRNA in all experiments was 100 nM.

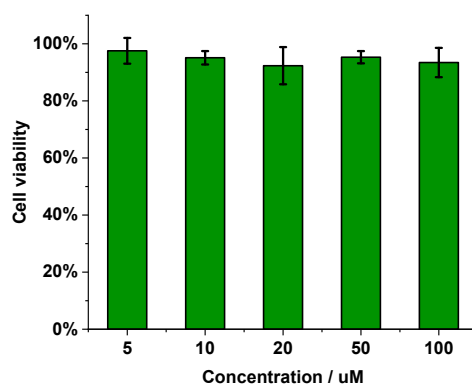


Figure S29. Cell viability of A549 cells induced with AAPS-HACD-UCNPs@c-siRNA at various concentrations under anaerobic incubation and 980 nm irradiation. The concentration of c-siRNA in all experiments was 100 nM.